Flow and clogging in a horizontal silo with a rotary obstacle

Cong-Cong Xu(徐聪聪), Qing-Fan Shi(史庆藩), Wei Liu(刘伟)[†], and Ning Zheng(郑宁)[‡]

School of Physics, Beijing Institute of Technology, Beijing 100081, *China*

(Received 28 April 2022; revised manuscript received 3 June 2022; accepted manuscript online 18 June 2022)

The external perturbation applied to a silo and the placement of an immobile obstacle before an exit are two common and effective ways to diminish clogging in the hopper/silo flow. Here, we incorporate the local perturbation into a fixed obstacle, and experimentally explore the effects of a rotary obstacle on clogging and the flowing characteristics in the horizontal silo flow driven by a conveyor belt. Even with a low spin rate, the total blocking probability that a particle constructs a stable blocking arch with its neighbors significantly drops. Correspondingly, the average flow rate of the particles through the exit abruptly rises, at least 1 order of magnitude better than that with an immobile obstacle and approaching the flow rate of continuous flow. The rotation enhances the breakage of clogging arches, which is responsible for improving the flowability in the horizontal silo. In addition, there always exists an optimal obstacle position at which the total blocking probability is minimal and the average flow rate peaks, regardless of the spin rate. Finally, clogging is relieved with the increase of the driving velocity of the conveyor belt, showing a "fast is fast" effect that is opposite to the "fast is slow" effect in other systems such as crowd evacuation and gravity-driven hoppers.

Keywords: granular flow, clogging, obstacle, rotation

PACS: 45.70.Mg, 47.57.Gc **DOI:** 10.1088/1674-1056/ac7a19

1. Introduction

Discrete substances passing through an exit/entrance are prone to clogging, which is ubiquitous across various scales in daily life and production: panic crowd evacuation,[1] particles discharging from a hopper or silo,[2] the thrombus formed in a blood vessel,[3] and micro-particles' agglomeration in constraints.[4] Clogging has both positive and negative sides, such as leaking stoppage or serious traffic jams. It is, therefore, of scientific and practical importance to investigate the clogging of particles through a bottleneck. Over the past decades, many constructive results clarify how clogging is affected by the shape and the size of an exit,[2,5–7] the shape, friction and softness of particles,[8–10] interstitial media,[11,12] the driving force,[13,14] and obstacles near an outlet.[15–17]

The clogging of particles usually originates from blocking arches before an exit. In order to alleviate clogging, two practical schemes are often applied to reduce the probability of arch formation or break a pre-existing arch. Exerting a global or a local perturbation, e.g., shaking a silo[18–24] or an exit,[25–28] is an effective method to destabilize blocking arches. As expected, the vibrations during the discharge can enhance the average flow rate. Alternatively, the placement of an obstacle before an outlet is another simpler way of improving the flow, especially suitable for situations in which vibrations are strictly prohibited.[29–37] An obstacle above the outlet at an appropriate position can increase the flux of particles from a silo noticeably,[29] and the probability that the flow is interrupted was lowered by 2 orders of magnitude.[16] Clogging suppression is attributed to a pressure decrease at the region of a blocking arch. Similarly, in the pedestrian[30–34] and the sheep herd evacuation,[35,36] there also exists optimal positioning of an obstacle, which decreases the evacuation time and stabilizes the longitudinal crowd waves, thus reducing the risk of trampling.

However, so far, obstacles in most studies are immobile, and study on how clogging is affected by a mobile obstacle still lacks. Here, we incorporate local perturbation into a fixed obstacle, and experimentally explore the effects of the rotary obstacle (i.e., the spin rate and the obstacle's position) and of the driving velocity on clogging and flowing characteristics in a horizontal silo driven by a conveyor belt. As the obstacle rotates even at a low spin rate, the total blocking probability is 15 times lower than that with an immobile obstacle, and the average flow rate of the system with the rotary obstacle can be increased by up to 1 order of magnitude. We borrow a model from a vibrated silo to estimate the probability of breaking a blocking arch by rotation. As with clogging in the system with a stationary obstacle, there also exists an optimal obstacle position where the total blocking probability is minimal and the average flow rate peaks. Finally, we confirm that a "fast is fast" effect still holds in the horizontal flow system with a rotary obstacle.

2. Experimental establishment

A monolayer of disk particles on a conveyor belt are driven through a narrow exit in front of which a rotary obstacle is placed. The particles in the upstream are supplemented

[†]Corresponding author. E-mail: liuwei73150@bit.edu.cn
[‡]Corresponding author. E-mail: ningzheng@bit.edu.cn

© 2023 Chinese Physical Society and IOP Publishing Ltd

by a circulation conveyor belt, basically keeping the particle's number before the exit unchanged; see Fig. 1(a).

The conveyor belt is 430 mm wide, around 39 times wider than a diameter of a particle (the diameter 11 mm). The boundary effect on the flow, thus, is negligible. A rotary gear-like obstacle is fixed before a small exit (see Fig. 1(b)). The external diameter of the gear is 19 mm, the length of a tooth is 5 mm, and the thickness of the gear is 4.5 mm. There are eight teeth evenly distributing the gear. The distance from the bottom of the obstacle to the exit is h, and the exit width is D.

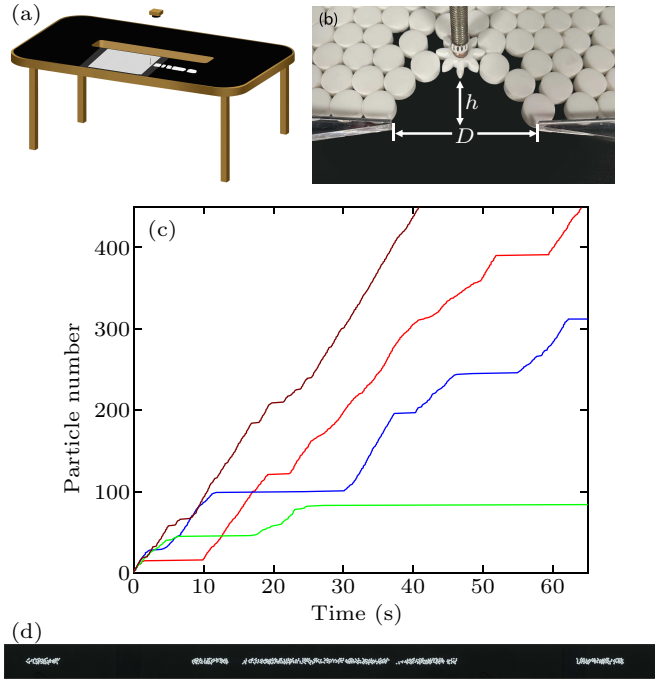


Fig. 1. (a) A schematic diagram of the experimental system. (b) An exit with a rotary gear-like obstacle. Inset at the top right-hand corner: geometry and shape of the gear-like obstacle. (c) Typical time evolutions of the number of particles discharging from a narrow exit. The plateaus in these curves show clogging durations. (d) A spatiotemporal image of particles crossing the exit. The horizontal direction in the spatiotemporal image indicating time, and the vertical direction is the width of the sampling window.

The rotary gear is driven by a regulating motor, and the spin rate of the gear can be tuned from 0 to 100 π/min. Approximately 2100 disks are used in the experiment. When these disks are driven through a small exit, some of them will constitute a blocking arch near the exit, causing a temporary or permanent clogging event. Because spontaneous unclogging often occurs due to the breakage of the blocking arch from the gear rotation and the belt shear, intermittent flow dominates, as illustrated in Fig. 1(c). We consider that the silo to experience long-lasting clogging when the discharge halts for more than 100 s, because it is rare that the silo can restart its discharge after such a duration. If such stable clogging happens, we use compressed air to destroy the blocking arch and resume the flow.

A camera is employed to record the space–time coordinate of each particle crossing the exit. A spatiotemporal image is obtained from the recorded video (see Fig. 1(d)), and the method was specified in the previous Ref. [38]. Through an imaging recognition for the spatiotemporal image, the time lapse of consecutive particles is extracted. We can define a clogging criterion and calculate the resulting clogging parameters on the basis of the time lapse of consecutive particles.

3. Results

3.1. Effects of the spin rate of an obstacle

The effects of the spin rate of a rotary obstacle on clogging are presented in this section, where the exit size D is 4.4 cm (i.e., $D/d = 4$, d the diameter of a disk particle), the distance h from the obstacle bottom to the exit is 4 cm and the driving velocity of the conveyor belt is kept at 5 cm/s. Because the rotation from the obstacle and the cyclic shear from the conveyor belt continuously break the blocking arches, the spontaneous unclogging stochastically occurs, which causes a giant fluctuation of the clogging time interval, and it is challenging to choose an appropriate time interval to define a clogging event. Fortunately, the issue has been solved in previous work.[35,38,39]

First, a complementary cumulative distribution function (CCDF) of the time interval Δt is extracted from the spatiotemporal image, as exhibited in Fig. 2(a). A power-law tail is seen in these distribution curves, $P(t \geq \Delta t) \propto \Delta t^{1-\alpha}$, which are also found in other scenarios such as with pedestrians, animals, gravity-driven silos and the horizontal silos.[35,39–41] We apply the Clauset–Shalizi–Newman method to fit the CCDF, and obtain the minimum time interval Δt_c from which the fit is valid, and the exponent of a power-law tail, α.[42]

The exponent α is an indicator used to judge whether a flowing system is inclined to clog or flow.[35,40] If $\alpha > 2$, the system finally tends to flow. Otherwise, the system is prone to clogging. As seen in Fig. 2(a), when the spin rate of the obstacle $\omega = 0$ (i.e., an immobile obstacle), the system tends to clog with a power-law exponent $\alpha = 1.55$ less than 2. While the obstacle rotates, α is greater than 2 for all spin rates, suggesting that discharge is continuous. We compare the value of the exponent α in various systems. $\alpha = 3.0$ ($\alpha = 4.0$) is for sheep passing through a small door without (with) an obstacle.[35] For robots through a narrow exit, $\alpha = 3.2$ is for a minimum number of robots.[39] When humans evacuate a room, three levels of competitiveness among crowds were studied. $\alpha = 6.8$ is for low competitiveness, $\alpha = 5.5$ is for middle competitiveness, and $\alpha = 4.2$ is for high competitiveness.[41] For a vibrated two-dimensional flat-bottomed vertical silo, $\alpha = 1.6$–2.2 at different vibration strengths.[40] In our horizontal silo with a rotary obstacle, α ranges from 1.55 to 2.85. It seems that the active agents that can take energy from their environment and drive themselves to move have a greater exponent α compared with passive particles when passing through a narrow exit.

The minimum time interval Δt_c is applied to determine clogging events. If $\Delta t < \Delta t_c$, the passage of particles is "flowing", otherwise "clogging" takes place. Two parameters, α and Δt_c, for all spin rates are shown in Table 1.

Table 1. Two parameters, α and Δt_c, for various spin rates.

Spin rate ω (rad/min)	Power-law exponent α	Δt_c (s)
0	1.55	0.25
10	3.05	0.25
20	2.83	0.25
30	2.72	0.25
40	2.73	0.25
50	2.85	0.25

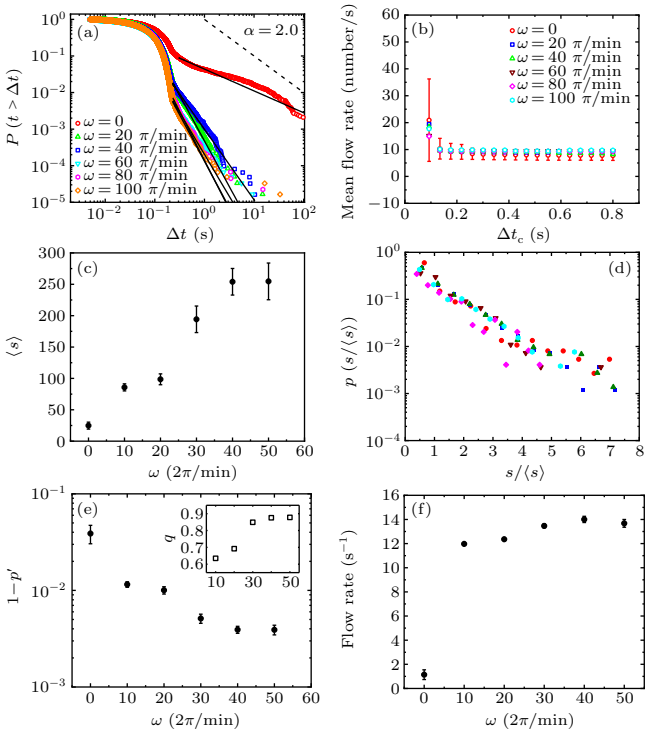


Fig. 2. (a) CCDFs of the time interval for various spin rates. Solid lines are power-law fits. The dashed line marked with $\alpha = 2.0$ is a boundary between clogging and flowing. (b) Mean flow rate inside avalanches vs. Δt_c. (c) Average avalanche size $\langle s \rangle$ vs. spin rate. (d) Rescaled histograms of the avalanche size for different spin rates. (e) Total blocking probability of a particle clogging the exit, $1 - p'$, vs. the spin rate ω. Inset: arch breakage probability q vs. spin rate ω. (f) Average flow rate, in units of number of particles per second, vs. the spin rate.

In addition, we can use another method to estimate Δt_c.[35,38] As shown in Fig. 2(b), the mean flow rate saturates at the range of $\Delta t_c = 0.15$ s–0.25 s, which is about the same size as that from the Clauset–Shalizi–Newman method. In the following statistics, 0.25 s is adopted as the minimum time interval used to define clogging.

After Δt_c is determined, an avalanche size s (i.e., the number of particles discharging between two consecutive clogging events) and the avalanche size distribution for each spin rate can be obtained accordingly. The average avalanche size $\langle s \rangle$ grows with an increase of ω, as shown in Fig. 2(c). By redefining $s^* = s/\langle s \rangle$, the rescaled avalanche sizes collapse together in an exponential form; see Fig. 2(d). Interestingly, the exponential form also exists in the flow of pedestrians, animals, or toy robots passing through a narrow door and in gravity-driven or a conveyor-driven silo flows,[35,38,39,41,43] appearing to be common across widely different systems.

As is well known, cloggin is caused by blocking arches consisting of particles moving through an exit. The probability of forming a blocking arch, and the probability of breaking the blocking arch already formed influence the presence of the arches. The factors, therefore, jointly determine the clogging time interval defining a clogging event, and further affect the avalanche size. In a previous study on clogging in a vibrated silo, the avalanche size $\langle s \rangle$ is given by[18]

$$\langle s \rangle = \frac{p + (1-p)q}{(1-p)(1-q)}, \tag{1}$$

where p is the probability of not forming a blocking arch when a particle passes through an exit with its neighboring particles, and q is the probability of breaking an existing arch due to the external perturbation, and can be seen as a measure of the "arch breakage probability". Equation (1) can be rewritten as

$$\langle s \rangle = \frac{p'}{1-p'}, \tag{2}$$

where $p' = p + (1-p)q$, the total probability of a particle not forming a blocking arch consists of two parts p and $(1-p)q$. p, as stated above, is the probability of not forming a blocking arch when a particle passes through an exit with its neighboring particles, and $(1-p)q$ denotes the probability that an existing arch is destroyed by the external perturbation. Then, $1-p'$ denotes the total blocking probability that a particle constructs a stable blocking arch with neighbors. According to Eq. (2), the dependence of the total blocking probability $1-p'$ on the spin rate ω is displayed. Figure 2(e) shows that $1-p'$ apparently drops with ω and is eventually saturated. The total blocking probability for $\omega = 0$ is 15 times higher than that for $\omega = 80\ \pi$/min. This indicates that the higher the spin rate, the less likely the presence of a stable arch at the exit. Finally, $1-p'$ is saturated with the increase of ω, implying that most of blocking arches disappear when the spin rate reaches a certain value.

Figure 2(a) also clearly shows that large amounts of clogging events with time intervals longer than 10 s appear when $\omega = 0$. However, with a slight increase of the spin rate, almost all clogging events with a long time interval vanish, suggesting that most persistent blocking arches have been eliminated. The rotation of the obstacle reasonably corresponds to the perturbation that breaks the clogging arch. The arch breakage probability q is, thus, closely related to the spin rate ω.

Next, we adopt the same assumption that p is not sensitive to the external perturbation as in the previous work,[18] because the rotation of the obstacle ($\omega < 1$ turn/s in all situations)

is also gentle. We attempt to estimate q based on this reasonable assumption. According to $p' = p + (1-p)q$, we can obtain $q = 1 - \frac{1-p'}{1-p}$ from the mean avalanche size $\langle s \rangle$ for the horizontal flow with and without the rotation as $p' = \frac{\langle s(\omega \neq 0) \rangle}{1+\langle s(\omega \neq 0) \rangle}$ and $p = \frac{\langle s(\omega=0) \rangle}{1+\langle s(\omega=0) \rangle}$, as shown in the inset of Fig. 2(e). It is not surprising that the ability of breaking an arch q increases with the spin rate since stronger rotation is expected to cause a larger perturbation to destabilize the same blocking arches. The saturation of q suggests that the arch-breaking ability approaches a limit as the spin rate goes beyond a threshold.

The average flow rate during the whole process can also be used to quantitatively characterize the intermittent flow and, notably, estimate the extent of clogging in the whole flow. The evacuation time for N particles moving out of the exit is defined as the duration between the escape of the first and of the Nth particle. The average flow rate is then given by $Q = 1/\langle \Delta t \rangle$, where the $\langle \Delta t \rangle$ is the mean lapse time, which is very different from the minimum time interval Δt_c.[41] Figure 2(f) shows that the average flow rate rises with the spin rate. When the obstacle starts to rotate even with a low spin rate, the average flow rate abruptly increases, up to 1 order of magnitude higher than that in the system with a stationary obstacle. The sharp increase in the average flow rate indicates that the slow rotation, namely, the weak arch-breaking ability, is able to effectively destroy most blocking arches lasting longer than 10 s, which is self-consistent with Fig. 2(a). Upon further increasing the spin rate, the average flow slowly increases and gradually saturates, suggesting that the increasing arch-breaking can break more clogging lasting longer than 10 s. However, the proportion of those subsequently broken clogs is very small among all clogs, and barely contributes to the average flow rate, resulting in flow saturation.

3.2. Distance from the bottom of the obstacle to the exit

The distance from the bottom of an obstacle to an exit, h, plays an important role in clogging and flowing. The blocking probability can be decreased up to 2 orders of magnitudes by the appropriate placement of an obstacle, but placing the obstacle too close to the exit will greatly increase the blocking probability.[15–17]

In this section, the size of the exit $D = 4.4$ cm, the driving velocity of the conveyor belt $V = 5$ cm/s, and the spin rate of the obstacle 60 π/min are fixed. By applying the same approach as in last section, we acquire CCDFs of the time interval for various distances h. Figure 3(a) clearly displays that the dependence of the power-law exponent α on the distance h is non-monotonic. At $h = 2$ cm, the distance is so close that clogging frequently takes place and results in $\alpha = 1.88$ even with a rotary obstacle. With an increase of h, α gradually grows until an optimal distance is achieved. When the obstacle is away from the exit with further increasing h, α decreases because the ability to destabilize the blocking arch from the obstacle constantly weakens; see Table 2. We also examine other spin rates and find that there always exists an optimal position where the exponent α peaks and the clogging probability reaches a minimum, which is very similar to the results for a stationary obstacle.[15–17,29] The mean flow rate is still used as the independent examination for the minimum time interval Δt_c, as shown in Fig. 3(b).

Table 2. Two parameters, α and Δt_c, for various positions of the obstacle, h.

Distance (cm)	Power-law exponent α	Δt_c (s)
2	1.88	1.0
3	3.99	0.3
4	2.74	0.3
5	2.51	0.3
6	2.21	0.3

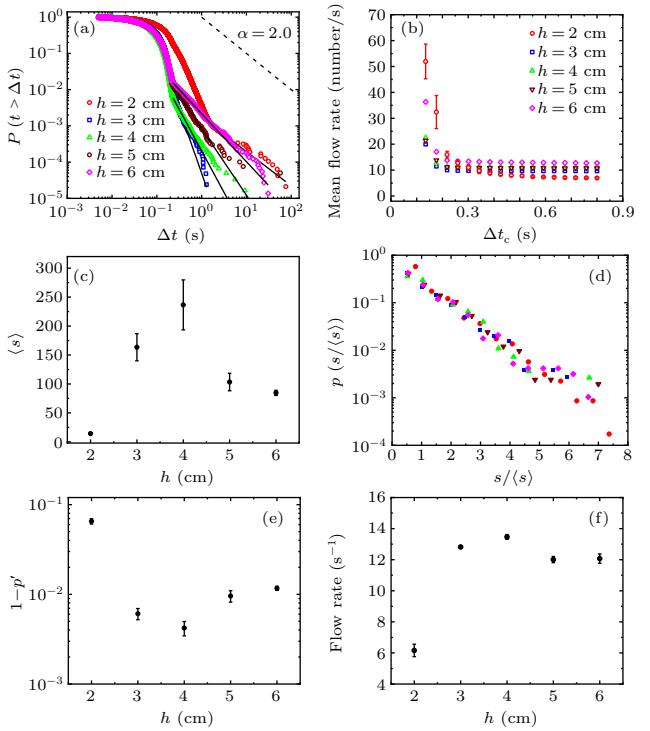


Fig. 3. (a) CCDFs of the time interval for various distances h. Solid lines are power-law fits. (b) Mean flow rate inside the avalanches vs. Δt_c. (c) Average avalanche size $\langle s \rangle$ vs. h. (d) Rescaled histograms of the avalanche size for different h. (e) Total blocking probability of a particle clogging the exit, $1 - p'$, vs. h. (f) Average flow rate vs. h.

In Fig. 3(c), the average avalanche size $\langle s \rangle$ also exhibits non-monotonic behavior with the distance h. At $h = 4$ cm, $\langle s \rangle$ rises to a peak, which is consistent with the maximum α in Fig. 3(a). Figure 3(d) shows that all distributions collapse into an exponential curve, being similar to Fig. 2(d) and further confirming the universality of the exponential law. With Eq. (2), the total blocking probability $1 - p'$ is extracted for different distances h, and the dependence is non-monotonic. At $h = 4$ cm, a minimum of $1 - p'$ is shown (see Fig. 3(e)). This suggests that the system is least likely to be clogged at $h = 4$ cm, and accordingly the average flow rate can be maximum at this point. Figure 3(f) shows that the average flow

rate indeed reaches a peak at $h = 4$ cm, and gradually saturates with the increase of the distance. The saturation of the average flow rate indicates that the obstacle far from the exit will no longer affect the flow rate.

3.3. Driving velocity of the conveyor belt

In most horizontal flows (i.e., the flow of sheep herds, pedestrians, and toy robots), the "fast is slow" effect, namely, an increase of the agents' velocity or the pressure instead causing more congestion near the entrance/exit, is prevalent.[39,41,44,45] However, we find that clogging in a conveyor belt system is relieved when increasing the driving velocity of the conveyor belt, suggesting the "fast is fast" behavior instead.[38] Whether the "fast is fast" effect still exists in the conveyor system with a rotary obstacle or the "fast is slow" comes back is an interesting question.

The exit size $D = 4.4$ cm, the spin rate $\omega = 40\ \pi/\text{min}$, and the distance $h = 3$ cm are fixed. The driving velocity V is tuned from 2 cm/s to 14 cm/s. The CCDFs of the time interval Δt for various driving velocities are plotted in Fig. 4(a). All exponents α except for that at $V = 2$ cm/s ($\alpha = 1.95$) are greater than 2, indicating the flowing status persists even with mild driving velocity. The mean flow rate saturates when the maximum Δt_c is more than 0.4 s; see Fig. 4(b). $\Delta t_c = 0.4$ s is used to differentiate flowing from clogging.

The average avalanche size $\langle s \rangle$ rises with the driving velocity V and finally approaches saturation. This trend resembles that in the conveyor belt flow without obstacles;[38] see Fig. 4(c). Similarly, the total blocking probability drops and finally reaches saturation, implying that the rotation has broken most blocking arches, as shown in Fig. 4(e). Similarly to in Figs. 2(d) and 3(d), the rescaled avalanche sizes collapse in an exponential form in Fig. 4(d). Finally, figure 4(f) shows that the average flow rate within the avalanches increases approximately linearly with the driving velocity, which further suggests that the rotation breaks most blocking arches and the flow is continuous; thus, the particle's velocity is associated with the driving velocity.

With the analysis of Figs. 4(c), 4(e), and 4(f), the issue at the start can be clarified. The conveyor-driven flow with a rotary obstacle still shows the "fast is fast" effect that appears in an obstacle-free conveyer belt system.

Figure 5 shows a clogging–flowing phase diagram in the ω–h space. It is clearly seen that most of the regions in the phase diagram are in the flowing state. Compared with the region caused by a stationary obstacle ($\omega = 0$), the clogging state tends to occur regardless of the position of the obstacle, which confirms that the rotary obstacle plays a crucial role in the transition from clogging to flowing. In addition, we also note that the position of the obstacle is also very critical to the two states. At $h = 2$ cm, where the distance between the obstacle and the exit is too close, the system always tends to clog, even if the obstacle rotates with a high spin rate. Otherwise, the system is inclined to flow with a low spin rate. This implies that the effect of the rotary obstacle on the flowing and the clogging state is very complex, and probably has both positive and negative influences simultaneously.

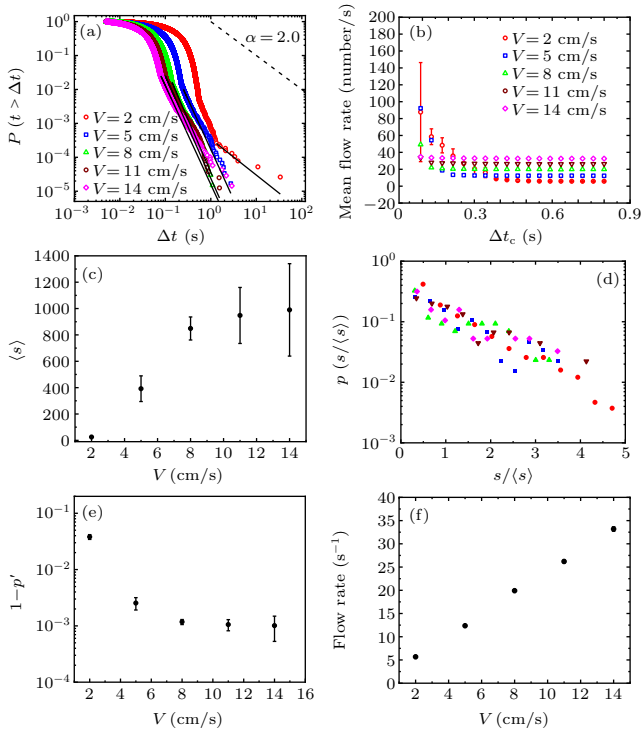


Fig. 4. (a) CCDFs of time interval for various driving velocities V. Solid lines are power-law fits. (b) Mean flow rate inside avalanches vs. Δt_c. (c) Average avalanche size vs. V. (d) Rescaled histograms of the avalanche size for various V. (e) Total blocking probability of a particle clogging the exit, $1 - p'$, vs. V. (f) The average flow rate vs. V.

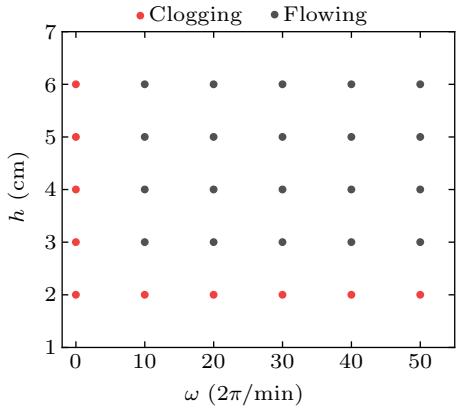


Fig. 5. A clogging–flowing phase diagram considering spin rate and distance space ($V = 5$ cm/s, $D = 4.4$ cm). Red dots indicate the clogging state, and black dots the flowing state.

4. Conclusion

In conclusion, the effects of the rotary obstacle and the driving velocity in a conveyor-belt-driven flow on clogging and flowing characteristics are experimentally explored. When the obstacle starts to rotate from rest, the flow experiences a transition from clogging to flowing status, and the total blocking probability correspondingly drops by more than

1 order of magnitude. The average flow rate rises sharply with a slight increase of the spin rate. Compared with the average flow rate in the system with an immobile obstacle, this one with a rotary obstacle can be increased by up to 1 order of magnitude, approaching the flow rate of continuous flow. This suggests that a low spin rate, namely a weak ability to destabilize clogging arches, already enabled most arches to be broken. It is also found that there exists an optimal position for a rotary obstacle to minimize the blocking probability, and this conclusion is applicable to all spin rates in our experiment.

In addition, the "fast is fast" effect still holds in the horizontal flow with a rotary obstacle, just as a conveyor belt system without any obstacles does. The rotary obstacle breaks most blocking arches, resulting in a nearly continuous particle flow, and thus the average flow rate increases linearly with driving velocity. Finally, we find that the rescaled avalanche sizes collapse together in exponential form, which also appears in the flow of pedestrians, animals, or robots and in gravity-driven or conveyor-driven silo flows, suggesting that clogging in most systems presumably shares a certain general property to form the scaling behavior, which appears to be more than a coincidence.

Acknowledgments

We appreciate Jon P. Johnson for their critical reading of this paper. Project supported by the National Natural Science Foundation of China (Grant No. 11974044).

References

[1] Helbing D, Farkas I and Vicsek T 2000 *Nature* **407** 487
[2] To K, Lai P Y and Pak H K 2001 *Phys. Rev. Lett.* **86** 71
[3] Zhou R and Chang H C 2005 *J. Colloid Interface Sci.***287** 647
[4] Bricard A, Caussin J B, Desreumaux N, Dauchot O and Bartolo D 2013 *Nature* **503** 95
[5] Masuda T, Nishinari K and Schadschneider A 2014 *Phys. Rev. Lett.* **112** 138701
[6] Saraf S and Franklin S V 2011 *Phys. Rev. E* **83** 030301
[7] Thomas C C and Durian D J 2013 *Phys. Rev. E* **87** 052201
[8] shour A, Wegner S, Trittel T, Börzsönyi T and Stannarius R 2017 *Soft Matter* **13** 402
[9] Tang J and Behringer R P 2016 *Europhys. Lett.***114** 34002
[10] Ashour A, Trittel T, Börzsönyi T and Stannarius R 2017 *Phys. Rev. Fluids* **2** 123302
[11] Koivisto J and Durian D J 2017 *Phys. Rev. E* **95** 032904
[12] Koivisto J, Korhonen M, Alava M, Ortiz C P, Durian D J and Puisto A 2017 *Soft Matter* **13** 7657
[13] Arévalo R, Zuriguel I, Maza D and Garcimartín A 2014 *Phys. Rev. E* **89** 042205
[14] Dorbolo S, Maquet L, Brandenbourger M, Ludewig F, Lumay G, Caps H, Vandewalle N, Rondia S, Mélard M, Loon J V, Dowson A and Vincent-Bonnieu S 2013 *Granul. Matter.* **15** 263
[15] Endo K, Reddy K A and Katsuragi H 2017 *Phys. Rev. Fluids* **2** 094302
[16] Zuriguel I, Janda A, Garcimartín A, Lozano C, Arévalo R and Maza D 2011 *Phys. Rev. Lett.* **107** 278001
[17] Lozano C, Janda A, Garcimartín A, Maza D and Zuriguel I 2012 *Phys. Rev. E* **86** 031306
[18] Mankoc C, Garcimartín A, Zuriguel I and Maza D 2009 *Phys. Rev. E* **80** 011309
[19] Wassgren C R, Hunt M L, Freese P J, Palamara J and Brennen C E 2002 *Phys. Fluids* **14** 3439
[20] Chen K, Stone M B, Barry R, Lohr M, McConville W, Klein K, Sheu B, Morss A J, Scheidemantel T and Schiffer P 2006 *Phys. Rev. E* **74** 011306
[21] Janda A, Maza D, Garcimartín A, Kolb E, Lanuza J and Clément E 2009 *Europhys. Lett.* **87** 24002
[22] Lindemann K and Dimon P 2000 *Phys. Rev. E* **62** 5420
[23] Wen P P, Zheng N, Nian J W, Li L S and Shi Q F 2015 *Sci. Rep.* **5** 9880
[24] Caitano R, Guerrero B V, González R E R, Zuriguel I and Garcimartín A 2021 *Phys. Rev. Lett.* **127** 148002
[25] To K and Tai H T 2017 *Phys. Rev. E* **96** 032906
[26] To K, Yen Y, Mo Y K and Huang J R 2019 *Phys. Rev. E* **100** 012906
[27] Hernández-Delfin D, Pongó T, To K, Börzsönyi T and Hidalgo R C 2020 *Phys. Rev. E* **102** 042902
[28] To K, Mo Y K, Pongó T and Börzsönyi T 2021 *Phys. Rev. E* **103** 062905
[29] Yang S C and Hsiau S S 2001 *Powder Technol.* **120** 244
[30] Yanagisawa D, Kimura A, Tomoeda A, Nishi R, Suma Y, Ohtsuka K and Nishinari K 2009 *Phys. Rev. E* **80** 036110
[31] Echeverría-Huarte I, Zuriguel I and Hidalgo R C 2020 *Phys. Rev. E* **102** 012907
[32] Feliciani C, Zuriguel I, Garcimartín A, Maza D and Nishinari K 2020 *Sci. Rep.* **10** 15947
[33] Chen Z H, Wu Z X and Guan J Y 2021 *Phys. Rev. E* **103** 062305
[34] Zhao Y X, Lu T T, Fu L B, Wu P and Li M F 2020 *Saf. Sci.* **122** 104517
[35] Garcimartín A, Pastor J M, Ferrer L M, Ramos J J, Martín-Gómez C and Zuriguel I 2015 *Phys. Rev. E* **91** 022808
[36] Zuriguel I, Olivares J, Pastor J M, Martín-Gómez C, Ferrer L M, Ramos J J and Garcimartín A 2016 *Phys. Rev. E* **94** 032302
[37] Areán M G, Boschan A, Cachile M A and Aguirre M A 2020 *Phys. Rev. E* **101** 022901
[38] Yu Q C, Zheng N and Shi Q F 2021 *Phys. Rev. E* **103** 052902
[39] Patterson G A, Fierens P I, Sangiuliano Jimka F, König P G, Garcimartín A, Zuriguel I, Pugnaloni L A and Parisi D R 2017 *Phys. Rev. Lett.* **119** 248301
[40] Zuriguel I, Parisi D R, Hidalgo R C, Lozano C, Janda A, Gago P A, Peralta J P, Ferrer L M, Pugnaloni L A, Clément E, Maza D, Pagonabarraga I and Garcimartín A 2014 *Sci. Rep.* **4** 7324
[41] Pastor J M, Garcimartín A, Gago P A, Peralta J P, Martín-Gómez C, Ferrer L, Maza D, Parisi D R, Pugnaloni L A and Zuriguel I 2015 *Phys. Rev. E* **92** 062817
[42] Clauset A, Shalizi C R and Newman M E J 2009 *SIAM Rev.* **51** 661
[43] Zuriguel I, Garcimartín A, Maza D, Pugnaloni L A and Pastor J M 2005 *Phys. Rev. E* **71** 051303
[44] Haghani M and Sarvi M 2018 *Transp. Res. Part B: Methodol.* **107** 253
[45] Sticco I M, Cornes F E, Frank G A and Dorso C O 2017 *Phys. Rev. E* **96** 052303